Analytical Methods

ROYAL SOCIETY OF CHEMISTRY

PAPER

View Article Online
View Journal | View Issue

Cite this: *Anal. Methods*, 2025, **17**, 5782

First-in-class hydrazone–pyrazoline sensors for selective detection of Zn^{2+}, Cd^{2+}, and Hg^{2+} in aqueous environments†

Alexander Ciupa *

Received 15th April 2025
Accepted 17th June 2025

DOI: 10.1039/d5ay00639b

rsc.li/methods

Six first-in-class hydrazone–pyrazoline fluorescent sensors that selectively detect Zn^{2+}, Cd^{2+}, and Hg^{2+} at three distinct wavelengths in aqueous environments are reported. These novel hybrid sensors are synthesized in just two steps from inexpensive, commercially available materials, enabling rapid generation and screening for desirable photophysical properties. Lead sensor **P1** was validated for *in situ* detection of group 12 metals in river and pond water using a portable, low-cost device. Crucially, this system enabled rapid, naked-eye detection of toxic metals directly in the environment without the need for expensive instrumentation or mains electricity. These findings establish a new direction in pyrazoline sensor research and set a high benchmark for future sensor development.

Introduction

The first three metals in group 12 of the periodic table are zinc, the second most abundant transition metal in the human body critical to life,[1] cadmium, a highly toxic industrial pollutant linked to numerous cancers,[2] and mercury, with well-established neurotoxicity.[3] The European Union (EU) maximum drinking water limits for cadmium and mercury are 44 nM and 5 nM respectively.[4] The World Health Organisation (WHO) has a recommended zinc drinking water limit of 46 μM.[5] The regular monitoring of group 12 metals in aqueous environments such as drinking water and external water courses is paramount. The ability to distinguish between Zn^{2+}, Cd^{2+}, and Hg^{2+} in aqueous environments is a major challenge requiring expensive and complex equipment not widely available, for example, ICP-MS. Fluorescence spectroscopy offers several advantages[6] over traditional techniques including high selectivity, low limits of detection (LoD), and rapid analysis. Fluorescent sensors are "turned on" when the analyte increases fluorescence emission (λ_{em})[7] or "turned off" when the analyte decreases λ_{em}.[8] Inhibition of photoinduced electron transfer (PET)[9] or the chelation enhancement effect (CHEF)[10] can increase λ_{em}. Decreased λ_{em} may result from fluorescence resonance energy transfer (FRET)[11] or chelation-enhanced quenching effect (CHEQ).[12] While numerous fluorescent sensors have been reported for Zn^{2+} and Cd^{2+},[13] few can differentiate between these metals at different λ_{em}.[14] The pyrazoline scaffold[15] (blue in Fig. 1) is highly advantageous due to its unique fluorescence properties[16] and modular structure from readily accessible chalcone precursors.[17] Chalcones, while utilized as precursors for pyrazolines, have also been reported to display useful sensing properties.[18] Pyridine is a well-established metal chelator often integrated into fluorescent sensors for Zn^{2+}, Hg^{2+} and Fe^{3+} detection.[19] Simple pyrazoline **A** displayed a "turn on" response only in the presence of Zn^{2+} and Cd^{2+};[20] **B** is a "turn on" sensor[21] for Fe^{3+}/Fe^{2+} whereas **C** displayed a "turn off" response in the presence of Fe^{3+}/Fe^{2+}.[21] Pyrazole **D** (red in Fig. 1)[22] demonstrated that an additional acetyl group greatly improved Zn^{2+}/Cd^{2+} selectivity. **A–D** reveal that structural complexity is not essential for complex functionality[20–22] highlighting the potential of these scaffolds in sensor development. During a recent pyrazoline synthesis study (see ESI S1†) side product **P1** was identified (Scheme 1), isolated, and discovered as a "turn on" sensor for Zn^{2+} at λ_{em} 560 nm and Cd^{2+} at 510 nm and a "turn off" sensor for Hg^{2+} at λ_{em} 460 nm. This unexpected side product is a highly attractive first-in-class hydrazone–pyrazoline multi-analyte group 12 sensor in aqueous environments.

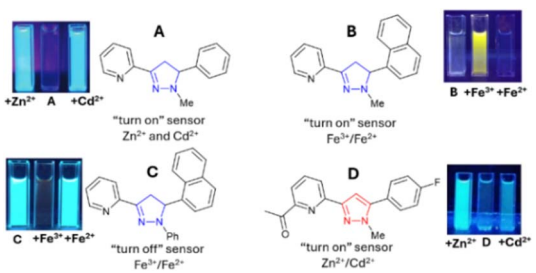

Fig. 1 Pyrazoline and pyrazole sensors; images reproduced from ref. 20–22 with permission from RSC.

Materials Innovation Factory, University of Liverpool, 51 Oxford Street, Liverpool L7 3NY, UK. E-mail: ciupa@liverpool.ac.uk

† Electronic supplementary information (ESI) available. See DOI: https://doi.org/10.1039/d5ay00639b

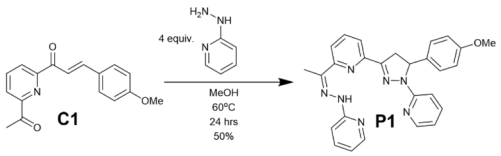

Scheme 1 Unexpected synthesis of side product **P1** from **C1**.

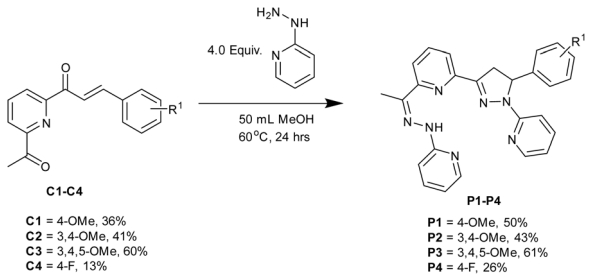

Scheme 2 Synthesis of hydrazone–pyrazoline series **P1–P4**.

Experimental

Chemicals and instruments

Chemicals, solvents and reagents were purchased from commercial sources and used without further purification. PE refers to petroleum ether, bp 40–60 °C. Spectroscopy was performed with CHROMASOLV® gradient grade acetonitrile for HPLC, ≥99.9%, from Sigma-Aldrich. The metal complexes used in this study were LiCl, NaCl, KCl, $CaCl_2$, $MgCl_2$, $CuCl_2$, $NiCl_2$, $ZnCl_2$, $CdCl_2$, $RuCl_3$, $CoCl_2$, $MnCl_2$, $PbCl_2$, $ZnCl_2$ and HgI_2.

UV/vis spectroscopy was performed on an Agilent Cary5000 using quartz cuvettes with a 1 cm pathlength using HPLC grade MeCN, in the 250–500 nm range with 0.2 s dwell time. Detector switchover occurred at 350 nm. FTIR spectroscopy was performed on a Bruker VERTEX 70 spectrometer. Fluorescence spectroscopy was performed on an Edinburgh Instruments FLS1000 with a xenon excitation source, 2 nm bandwidths for both excitation and emission monochromators, a scan speed of 1 nm and a dwell time of 0.2 s. Fluorescence quartz cuvettes with a 1 cm pathlength were used throughout with HPLC grade MeCN. A 100 watt 365 nm Analytik Jena high intensity UV lamp was used to image the sensors.

Synthesis of chalcones C1–C4

The following general procedure was followed (see the ESI† for more detailed information), using a method adapted from a previous synthesis,[22] 6 mmol 2,6-acetylpyridine was added to a stirred solution of 3.0 mmol aldehyde in MeOH followed by the addition of 3.0 mmol NaOH and stirring was continued at room temperature. After 24 hours the precipitate was filtered, washed with copious amounts of cold H_2O collected and dried to afford the desired chalcone without further purification.

Synthesis of hydrazone–pyrazolines P1–P6

The following general procedure was followed: 4.0 mmol of 2-hydrazinopyridine was added to a stirred solution of 1.0 mmol of required chalcone in 50 mL MeOH and heated to 60 °C. After 24 hours, the solvent was removed under reduced pressure, 100 mL H_2O was added and it was extracted into 3 × 50 mL ethyl acetate. The ethyl acetate fractions were combined and the solvent was removed under reduced pressure to give an oil which was then purified by column chromatography with 6 : 4 ethyl acetate : petroleum ether to afford the desired product.

Results and discussion

Chalcones **C1–C4** were prepared using a previous procedure[22] in acceptable yields (13–60%). A direct chalcone to hydrazone–pyrazoline synthesis was developed to give novel compounds **P1–P4** (Scheme 2) in good yield (26–61%).

This two-step synthesis from inexpensive commercially available starting materials unlocks a new class of previously unexplored pyrazoline sensors. Furthermore, the modular nature of the pyrazoline scaffold enables a high degree of modification unlocking a deeper understanding of their sensing properties. With four novel hydrazone–pyrazolines in hand, we investigated their photophysical properties against the group 12 metals using well-established protocols.[22–24] UV/vis studies confirmed that **P1** undergoes chelation with both Zn^{2+} and Cd^{2+} with the formation of a new band at 285 and 290 nm respectively (Fig. 2A and B). A ^{1}H NMR titration study for **P3** in the presence of the group 12 metals indicated broadening and downfield movement for multiple signals (Fig. 2C for **P3** with Hg^{2+}). The broad singlet at 8.54 ppm attributed to the hydrazone proton H^a shifted to 9.31 ppm on the addition of 2.0 equivalents Hg^{2+}. Significant shifts in the remaining protons were also observed; for example, the pyridine signal from H^b moved from 7.79 ppm to 7.99 pm and the aryl singlet for H^c moved from 6.54 to 6.68 ppm. This is a well-established

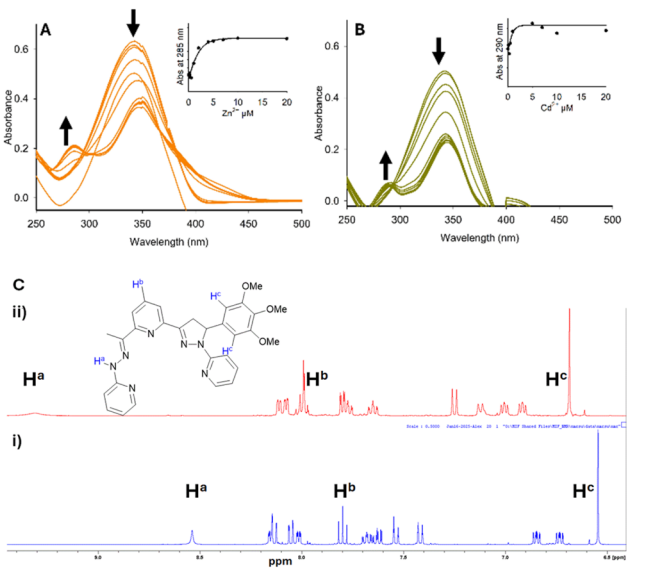

Fig. 2 UV/vis study of **P1** (20 µM, MeCN) with 0–20 equivalents of Zn^{2+} (panel A) and Cd^{2+} (panel B). ^{1}H NMR studies of **P3** (9 µM, deuterated MeCN), (panel C) (i) **P3** only and (ii) +2.0 equivalents of Hg^{2+}.

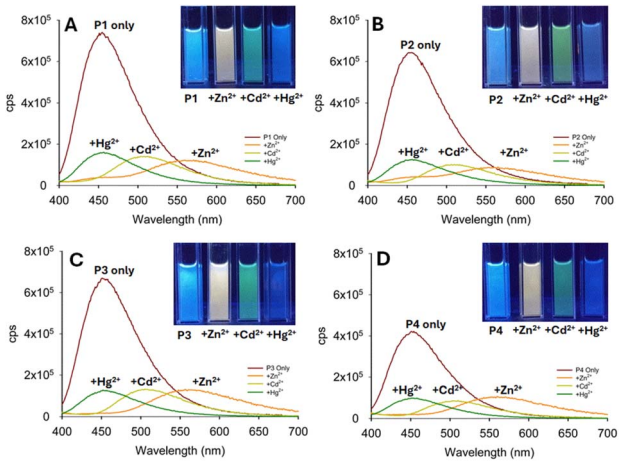

Fig. 3 Fluorescence studies of **P1–P4** (A–D) 15 μM, 7 : 3 MeCN : H_2O at λ_{ex} 285 nm, on addition of 5.0 equivalents of the indicated metal; cps is counts per second. Cuvette images were obtained under the irradiation of a 100 W λ_{ex} 365 nm lamp.

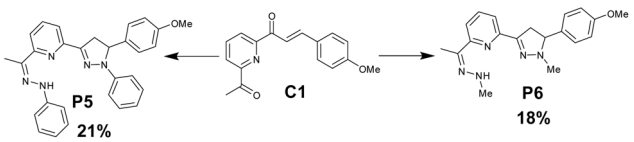

Scheme 3 Synthesis of hydrazone–pyrazoline **P5–P6**.

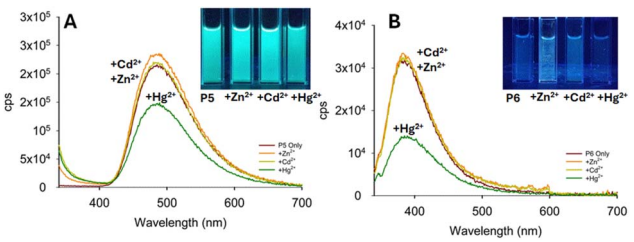

Fig. 4 Fluorescence studies of **P5** (A) and **P6** (B) 15 μM, 7 : 3 MeCN : H_2O at λ_{ex} 285 nm; cps is counts per second. Cuvette images were obtained under the irradiation of a 100 W λ_{ex} 365 nm lamp.

observation with previous pyrazoline sensors undergoing chelation.[20–23,24a,b]

The fluorescence response of **P1** (φ_f 4.0%, τ 3.4 ns) was confirmed with the formation of new emission bands at 560 nm with Zn^{2+} (φ_f 1.0%, τ 14 ns) and 510 nm with Cd^{2+} (φ_f 1.0%, τ 13 ns) in 7 : 3 MeCN : H_2O (Fig. 3A). On addition of Hg^{2+} a "turn off" response at λ_{em} 460 nm (φ_f < 1.0% τ 4.0 ns) is observed. Of note is that the response is retained in an aqueous solution demonstrating the real-world application of this sensor. A similar fluorescence profile was obtained with **P2–P4** suggesting that substitution on the aryl ring was well-tolerated a range of both electron donating and electron withdrawing substituents. To determine the importance of hydrazone, two further pyrazolines were synthesised; **P5** using phenyl hydrazine and **P6** with methyl hydrazine (Scheme 3). **P5** displayed no

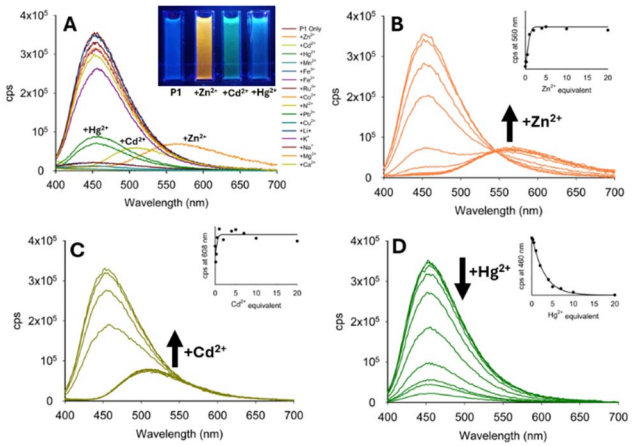

Fig. 5 (A) Fluorescence studies of **P1** 15 μM, 7 : 3 MeCN : H_2O at λ_{ex} 285 nm. (Panels B–D) Titration studies for Zn^{2+}, Cd^{2+} and Hg^{2+}, respectively; cps is counts per second. Cuvette images were obtained under the irradiation of a 100 W λ_{ex} 365 nm lamp.

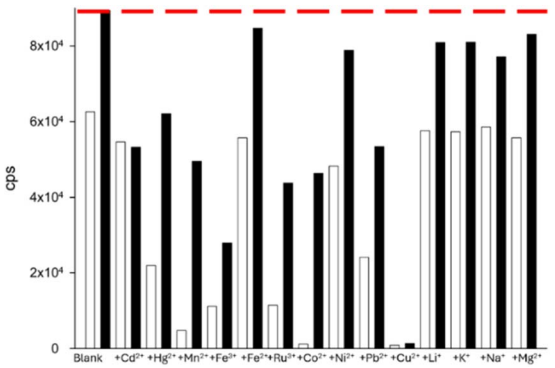

Fig. 6 Competition assay for **P1** with Zn^{2+} in the presence of a range of interferents. The white bar represents the sensor (20 μM, 7 : 3 MeCN : H_2O) with 5.0 equiv. of the indicated cation; the black bars are the same with 5.0 equiv. of Zn^{2+} after equilibrating for 2 min. λ_{ex} 285 nm with λ_{em} 560 nm; the red line indicates the "turn on" response with Zn^{2+} only, and cps is counts per second.

distinguishing features suggesting that the pyridine ring in **P1–P4** was critical for group 12 selectivity. **P6** with methyl units displayed insignificant fluorescence on addition of the group 12 metals suggesting that an aromatic unit was required. The contrast between **P1** and **P5** is striking confirming that pyridine units are essential for group 12 selectivity (Fig. 4).

P1 was selected as the lead compound and submitted for further investigation. A titration study confirmed λ_{em} at 560 nm (yellow emission) which peaked with 5.0 equivalents of Zn^{2+} (Fig. 5B). A Zn^{2+} limit of detection (LoD) of 6.4 μM was calculated which is well below the WHO recommended drinking water limit. A similar study with Cd^{2+} confirmed λ_{em} at 510 nm (green emission) which reached a plateau with 5.0 equivalents of Cd^{2+} (LoD 2.4 μM). The 50 nm difference in λ_{em} between Zn^{2+} and Cd^{2+} is significant with very few examples reporting such a distinction between two group 12 metals.[14] To our surprise Hg^{2+} generated an opposite response, a "turn off" response, with a decrease in λ_{em} at 460 nm, Hg^{2+} LoD 10.0 μM. These LoD

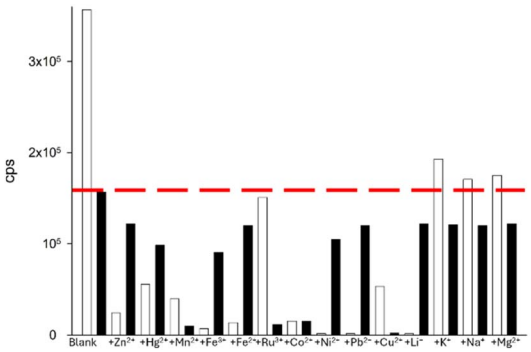

Fig. 7 Competition assay for **P1** with Cd^{2+} in the presence of a range of interferents. The white bar represents the sensor (20 μM, 7 : 3 MeCN : H_2O) with 5.0 equiv. of the indicated cation; black bars are the same with 5.0 equiv. of Cd^{2+} after equilibrating for 2 min. λ_{ex} 285 nm with λ_{em} 500 nm.

values agree with those of previously reported pyrazoline sensors for Zn^{2+} and Cd^{2+} (ESI S6†). Competition assays were performed to determine the response of **P1** in the presence of a range of interferents (Fig. 6 for **P1** with Zn^{2+}).

Several paramagnetic metals including Fe^{3+}, Ru^{3+}, Co^{2+}, and noticeably Cu^{2+} disrupted the "turn on" response to Zn^{2+} at 560 nm (Fig. 6). This is a common phenomenon for pyrazolines with paramagnetic metals.[13b,c,22,23] Interestingly, the biological group 1 and 2 metals, Li^+, K^+, Na^+ and Mg^{2+}, resulted in very minor disruption suggesting that **P1** could be used for the monitoring of Zn^{2+} in living systems high in these metals, an active research area.[13a,26] A similar profile was observed with Cd^{2+}; paramagnetic metals Mn^{2+}, Ru^{3+}, Co^{2+} and Cu^{2+} hampered λ_{em} 510 nm but a good response remained with the group 1 and 2 metals (Fig. 7). A further assay of **P1** with Hg^{2+} showed that paramagnetic metals disrupted the "turn off" response (Fig. 8). Under these conditions, the group 1 and 2 metals did not significantly influence the "turn off" response to Hg^{2+} suggesting that **P1** could be a useful sensor for the "turn on" detection of Zn^{2+} at 560 nm and the "turn off" detection of Hg^{2+} at 460 nm in biological systems.

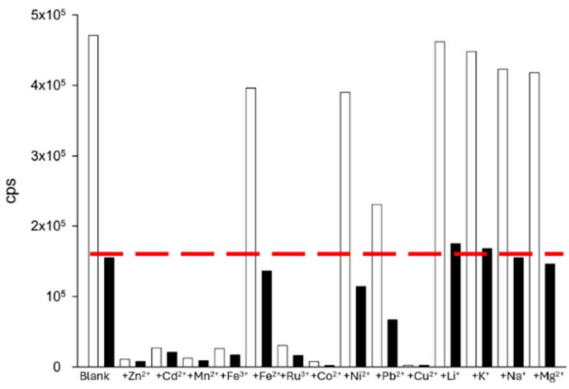

Fig. 8 Competition assay for **P1** with Hg^{2+} in the presence of a range of interferents. The white bar represents the sensor (20 μM, 7 : 3 MeCN : H_2O) with 5.0 equiv. of the indicated cation; the black bars are the same with 5.0 equiv. of Hg^{2+} after equilibrating for 2 min. λ_{ex} 285 nm with λ_{em} 460 nm; the red line indicates the "turn off" response with Hg^{2+} only.

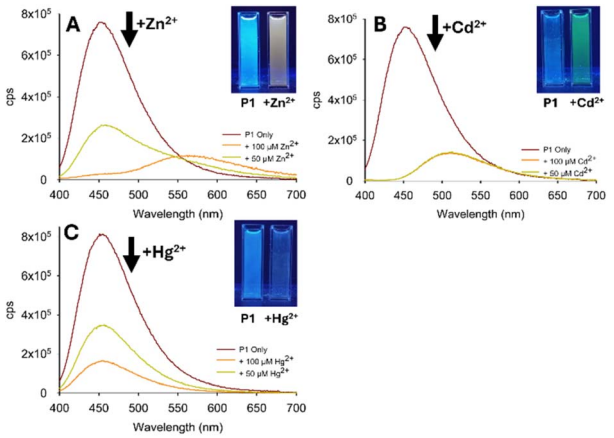

Fig. 9 Group 12 metal triggered fluorescence response of **P1** (20 μM, 7 : 3 MeCN : H_2O) in tap water; Zn^{2+} (panel A), Cd^{2+} (panel B) and Hg^{2+} (panel C). Cuvette images under the irradiation of the 100 W λ_{ex} 365 nm lamp.

To determine the real-world application of **P1** in large-scale monitoring, several studies of a variety of water sources were conducted including drinking water (tap and mineral water see Fig. 9 and ESI S5†). A strong response to 100 μM Zn^{2+} in tap water (Fig. 9) with a visible colour change from blue to yellow was observed at λ_{ex} 365 nm (Fig. 9A inset). A similar study with Cd^{2+} in tap water produced a more noticeable response at 50 μM Cd^{2+} (Fig. 9B) and a green colour change under λ_{ex} 365 nm irradiation (Fig. 9B inset). The "turn off" response to Hg^{2+} was detectable in tap water (Fig. 9C) with a reduction in λ_{em} at 460 nm with both 50 μM and 100 μM Hg^{2+}. Mineral water (see ESI S5†) yielded a comparable result. The visible colour change on the addition of Zn^{2+} (yellow), Cd^{2+} (green) and Hg^{2+} (blue) suggests that **P1** could form a prototype for a low-cost and portable field-based device. A low-cost prototype was constructed consisting of a portable excitation source and a suitable dark box (ESI S8†).[25] Samples from two environmental

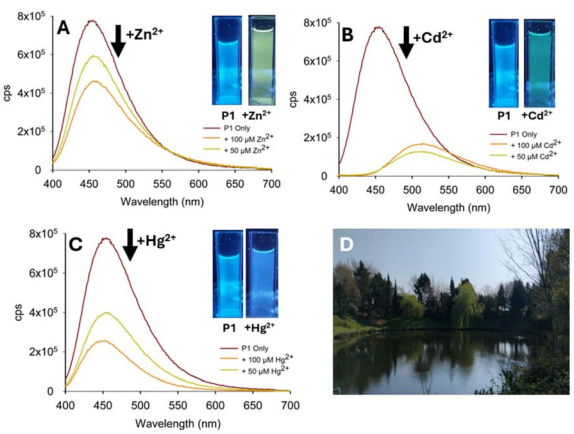

Fig. 10 Group 12 metal triggered fluorescence response of **P1** (20 μM, 7 : 3 MeCN : H_2O) in pond water; $+Zn^{2+}$ (panel A), $+Cd^{2+}$ (panel B), $+Hg^{2+}$ (panel C) and location (D).

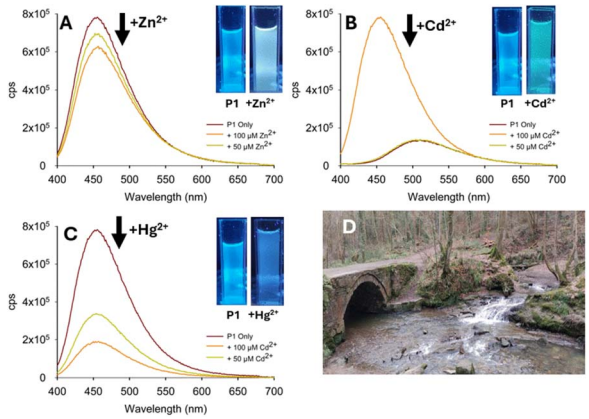

Fig. 11 Group 12 metal triggered fluorescence response of **P1** (20 μM, 7 : 3 MeCN : H_2O) in river water; $+Zn^{2+}$ (panel A), $+Cd^{2+}$ (panel B), $+Hg^{2+}$ (panel C) and location (D).

locations (river and pond water) were taken and analysed in the laboratory and *in situ* using a portable device (Fig. 10 for pond water).

At two different concentrations, 50 μM and 100 μM of Zn^{2+}, Cd^{2+}, and Hg^{2+}, a fluorescence response was triggered analogous to the drinking water study. The decrease in λ_{em} with Zn^{2+} (Fig. 10A) was less than expected possibly due to additional interferents present in the environment, possibly sediment or bacteria (Fig. 10A). In the presence of Cd^{2+} the change in λ_{em} is noticeable and a visible change to green is observed (Fig. 10B inset). A decrease in λ_{em} at 460 nm was observed on addition of Hg^{2+} (Fig. 10C inset) confirming that **P1** can distinguish Cd^{2+} from Hg^{2+} in the field that can be observed with the naked eye. A similar result was obtained in river water (Fig. 11). This study confirmed that **P1** can be used outside of a laboratory environment with naked eye detection of the group 12 metals in both stagnant pond and free flowing river waters. To confirm the robustness of **P1**, a reversibility study was performed which confirmed that **P1** can be used for multiple cycles for Zn^{2+} detection (Fig. 12A). The proposed binding mechanism of **P1** with Zn^{2+} (Fig. 12B) is 1 : 1 and agrees with previous studies on **A–D** and the Job plot (ESI S7†).[20–23] While hydrazone units have been incorporated into multi-analyte fluorescent sensors previously,[27] **P1–P4** are the first reported sensors combining hydrazone and pyrazoline units which distinguish Zn^{2+}, Cd^{2+}, and Hg^{2+} at different λ_{em} in aqueous environments.

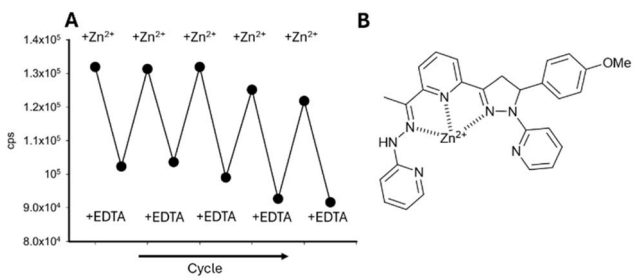

Fig. 12 A reversibility study for **P1** in the presence of multiple cycles of Zn^{2+} and EDTA (panel A) and the proposed binding mode of **P1** with Zn^{2+} (panel B).

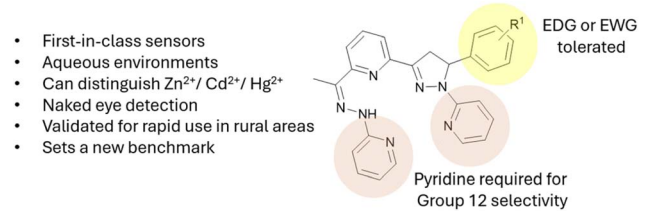

Fig. 13 Summary of **P1–P6**; EDG is the electron donating group and EWG is the electron withdrawing group.

Conclusions

Six first-in-class hydrazone–pyrazoline sensors were synthesised with **P1–P4** displaying excellent selectivity towards group 12 metals. The aryl ring was well-tolerated to both electron donating and withdrawing substituents; however, substitution of pyridine for a phenyl unit in **P5** abolished group 12 selectivity (Fig. 13). Substitution of the aryl ring on hydrazone and pyrazoline for methyl units in **P6** significantly disrupted the fluorescence intensity. **P1** was selected for further investigation and while a few heavy metals were significant interferents to the fluorescent response for **P1**, its ability to detect group 12 metals in real-world samples was confirmed. Combining **P1** with a low-cost portable device enabled rapid visual detection by the naked eye of the 12 metals in rural environments without expensive apparatus or mains electricity. The group 1 and 2 metals exhibited very little influence on the fluorescence response indicating that **P1** could also be a highly useful sensor for the selective detection of Zn^{2+} and Hg^{2+} in biological systems; for example cell culture and living systems.[26] This highly unexpected discovery establishes a new subset of pyrazoline sensors, hydrazone–pyrazoline hybrid sensors. These hybrid sensors composed of both hydrazone and pyrazoline functional units set a high benchmark for future group 12 sensors. Further work is underway to transform this discovery into a second generation of sensors that retain the group 12 metal selectivity of **P1** but with improved properties (increased λ_{em} intensity and reduced interference). The high tolerance of the aryl R^1 group to substitution enables the attachment of these sensors to solid substrates as reported previously by Magri *et al.*[28] This provides valuable applications for enhanced sensor design and molecular logic gate development.[29] These are priority objectives for ongoing work and will be reported in due course.

Data availability

The data supporting this article have been included as part of the ESI.†

Author contributions

Alexander Ciupa designed, synthesized, characterised, and performed all spectroscopy studies and authored the manuscript.

Conflicts of interest

There are no conflicts to declare.

Acknowledgements

The author acknowledges Steven Robinson for assistance with time-of-flight high resolution mass spectrometry and Krzysztof Pawlak for assistance with fluorescence spectroscopy. Emily Cunliffe is acknowledged for valuable discussions. This work made use of shared equipment located at the Materials Innovation Factory, created as part of the UK Research Partnership Innovation Fund (Research England) and co-funded by the Sir Henry Royce Institute.

References

1 C. T. Chasapis, C. A. Spiliopoulou, A. C. Loutsidou and M. E. Stefanidou, *Arch. Toxicol.*, 2012, **86**, 521.
2 G. Genchi, S. M. Sinicropi, G. Lauria, A. Carocci and A. Catalano, *Int. J. Environ. Res. Public Health*, 2020, **17**, 3782.
3 Y. S. Wu, A. I. Osman, M. Hosny, A. M. Elgarahy, A. S. Eltaweil, D. W. Rooney, Z. Chen, N. S. Rahim, M. Sekar, S. C. B. Gopinath, N. N. Mat Rani, K. Batumalaie and P. S. Yap, *ACS Omega*, 2024, **9**, 5100.
4 *Directive (EU) 2020/2184 Of The European Parliament And Of The Council of 16 December 2020, on the quality of water intended for human consumption*, 2015, **http://data.europa.eu/eli/dir/2020/2184/**.
5 *Zinc in Drinking-water, WHO/SDE/WSH/03.04/17*, **https://cdn.who.int/media/docs/default-source/wash-documents/wash-chemicals/zinc.pdf?sfvrsn=9529d066_4**.
6 H. N. Kim, W. X. Ren, J. S. Kim and J. Yoon, *Chem. Soc. Rev.*, 2012, **41**, 3210.
7 G. Wu, M. Li, J. Zhu, K. W. Chiu Lai, Q. Tong and F. Lu, *RSC Adv.*, 2016, **6**, 100696.
8 S. Manickam and S. K. Lyer, *RSC Adv.*, 2020, **10**, 11791.
9 H. Nui, J. Liu, H. M. O'Connor, T. Gunnlaugsson, T. D. James and H. Zhang, *Chem. Soc. Rev.*, 2023, **52**, 2322.
10 J. W. Nugent, H. Lee, H.-S. Lee, J. H. Reibenspies and R. D. Hancock, *Chem. Commun.*, 2013, **49**, 9749.
11 L. G. T. A. Duarte, F. L. Coelho, J. C. Germino, G. G. da Costa, J. F. Berbigier, F. S. Rodembusch and T. D. Z. Atvars, *Dyes Pigm.*, 2020, **181**, 108566.
12 L. Wu, C. Huang, B. P. Emery, A. C. Sedgwick, S. D. Bull, X. P. He, H. Tian, J. Yoon, J. L. Sessler and T. D. James, *Chem. Soc. Rev.*, 2020, **49**, 5110.
13 Selected examples: (*a*) Z. Zhang, F.-W. Wang, S.-Q. Wang, F. Ge, B.-X. Zhao and J.-Y. Miao, *Org. Biomol. Chem.*, 2012, **10**, 8640; (*b*) Z. L. Gong, F. Ge and B.-X. Zhao, *Sens. Actuators, B.*, 2011, **159**, 148; (*c*) M. M. Li, F. Wu, X. Y. Wang, T. T. Zhang, Y. Wu, Y. Xiao, J. Y. Miao and B.-X. Zhao, *Anal. Chim. Acta*, 2014, **826**, 77.
14 Selected examples: (*a*) Z. Xu, K.-H. Baek, H. N. Kim, J. Cui, X. Qian, D. R. Spring, I. Shin and J. Yoon, *J. Am. Chem. Soc.*, 2010, **132**, 601; (*b*) Y. Tan, J. Gao, J. Yu, Z. Wang, Y. Cui, Y. Yang and G. Qian, *Dalton Trans.*, 2013, **42**, 11465; (*c*) G. Tian, Y.-Z. Han and Q. Yang, *J. Mol. Struct.*, 2023, **1273**, 134341.
15 B. Varghese, S. N. Al-Busa, F. O. Suliman and S. M. Z. Al-Kindy, *RSC Adv.*, 2017, **7**, 46999.
16 H. El Karout, C. Labassi, K. Waszkowska, N. Fournier-le Ray, R. Gatri, F. Gauffre, A. Fihey, B. Sahraoui and J.-L. Fillaut, *New J. Chem.*, 2024, **48**, 18709.
17 A. Ciupa, P. A. De Bank, M. F. Mahon, P. J. Wood and L. Caggiano, *MedChemComm*, 2013, **4**, 956.
18 Selected examples: (*a*) S. A. Khan, M. Z. Alam, M. Mohasin, S. Ahmad, U. Salma, H. Parveen, S. Mukhtar, M. Al-Anazi, F. A. Alotaibi and M. A. Abdelaziz, *J. Fluoresc.*, 2024, **34**, 723; (*b*) S. Prajapati, P. Sinha, S. Hindore and S. Jana, *Spectrochim. Acta, Part A*, 2023, **287**, 122107; (*c*) L. E. Santos-Figueroa, A. Llopis-Lorente, S. Royo, F. Sancenón, R. Martínez-Máñez, A. M. Costero, S. Gil and M. Parra, *ChemPlusChem*, 2015, **80**, 800.
19 Selected examples: (*a*) M. Z. Alam, S. Ahmad, A. Alimuddin and S. A. Khan, *J. Fluoresc.*, 2025, **35**(3), 1241; (*b*) M. Z. Alam, M. Mohasin, S. Ahmad, U. Salma and S. A. Khan, *J. Coord. Chem.*, 2025, **48**, 367; (*c*) M. Mohasin, M. Z. Alam, S. Ahmad, U. Salma, Q. Ullah and S. A. Khan, *J. Mol. Struct.*, 2025, **1336**, 142034.
20 A. Ciupa, M. F. Mahon, P. A. De Bank and L. Caggiano, *Org. Biomol. Chem.*, 2012, **10**, 8753.
21 A. Ciupa, *RSC Adv.*, 2024, **14**, 34918.
22 A. Ciupa, *RSC Adv.*, 2024, **14**, 3519.
23 A. Ciupa, *New J. Chem.*, 2024, **48**, 13900.
24 Selected examples: (*a*) A. Sahana, A. Banerjee, S. Das, S. Lohar, D. Karak, B. Sarkar, S. K. Mukhopadhyay, A. K. Mukherjee and D. Das, *Org. Biomol. Chem.*, 2011, **9**, 5523; (*b*) S. Santhoshkumar, K. Velmurugan, J. Prabhu, G. Radhakrishnan and R. Nandhakumar, *Inorg. Chim. Acta*, 2016, **439**, 105; (*c*) N. Bhuvanesh, S. Suresh, K. Kannan, V. R. Kannan, N. Maroli, P. Kolandaivel and R. Nandhakumar, *New J. Chem.*, 2019, **43**, 2519; (*d*) Y. Mise, K. Imato, T. Ogi, N. Tsunoji and Y. Ooyama, *New J. Chem.*, 2021, **45**, 4164; (*e*) G. Mun, S. H. Jung, A. Ahn, S. S. Lee, M. Y. Choi, D. H. Kim, J.-Y. Kim and J. H. Jung, *RSC Adv.*, 2016, **6**, 53912.
25 R. Iftikhar, I. Parveen, A. Ayesha, A. Mazhar, M. S. Iqbal, G. M. Kamal, F. Hafeez, A. L. Pang and M. Ahmadipour, *J. Environ. Chem. Eng.*, 2023, **11**, 109030.
26 Selected examples: (*a*) S. Melo-Hernández, M. Camila Ríos and J. Portilla, *RSC Adv.*, 2024, **14**, 39230; (*b*) Y. Y. Gao, J. He, X.-H. Li, J.-H. Li, H. Wu, T. Wen, J. Li, G.-F. Hao and J. Yoon, *Chem. Soc. Rev.*, 2024, **53**, 6992.
27 Selected examples: (*a*) X. Su and I. Aprahamian, *Chem. Soc. Rev.*, 2014, **43**, 1963; (*b*) W. N. Wu, H. Wu, Y. Wang, X. J. Mao, B. Z. Liu, X. L. Zhao, Z. Q. Xu, Y. C. Fan and Z. H. Xu, *RSC Adv.*, 2018, **8**, 5640; (*c*) Y. Yang, W. W. Wang, W. Z. Xue, W. N. Wu, X. L Zhao, Z. Q. Xu, Y. C. Fan and Z. H. Xu, *J. Lumin.*, 2019, **212**, 191; (*d*) A. Ciupa, *RSC Adv.*, 2025, **15**, 3465.
28 N. Zerafa, M. Cini and D. C. Magri, *Mol. Syst. Des. Eng.*, 2021, **6**, 93.
29 A. Ciupa, *RSC Adv.*, 2025, **15**, 10565.